Hindawi
Advances in Civil Engineering
Volume 2021, Article ID 6615224, 11 pages
https://doi.org/10.1155/2021/6615224

Research Article

The Anti sliding Mechanism of Adjacent Pile-Anchor Structure considering Traffic Load on Slope Top

Danfeng Li[1,2] **and Zhuojie Zhang**[1,2]

[1]*State Key Laboratory of Mechanical Behavior and System Safety of Traffic Engineering Structures, Shijiazhuang Tiedao University, Shijiazhuang 050043, China*
[2]*School of Civil Engineering, Shijiazhuang Tiedao University, Shijiazhuang, Hebei 050043, China*

Correspondence should be addressed to Zhuojie Zhang; zhangzhuojie@stdu.edu.cn

Received 23 November 2020; Revised 24 August 2021; Accepted 24 September 2021; Published 8 October 2021

Academic Editor: Khalid Abdel-Rahman

In view of the fact that the anti sliding effect analysis of the current anchor cable and anti slide pile structure is not yet complete, research on the synergy mechanism of adjacent pile-anchor composite structures under traffic load is carried out. Firstly, a free vibration analysis for the slope dynamic model is carried out by using a three-dimensional finite element numerical simulation method. By improving the slope boundary conditions of time-domain analysis, the time-domain equation of the dynamic model of traffic load acting on the top of the slope is solved accurately, and the response law of the internal force of the pile anchor composite structure is also described. The mechanism by which the pile anchor composite structure resists against the slope sliding through the internal force increment is proposed: this internal force increment is estimated to be 73.4%, while that of anchor cable is 26.6%. The composite structure presents the coordinated sharing for sliding force. The internal force of the lower row of anchor cables is 89.48 kN larger than that of the upper row, and the internal force increment is four times larger, indicating that the lower anchor cable is more effective in slope reinforcement. As the deformation at the top of the slope is greater, the prestress of the upper anchor cable should be increased to avoid the "chain failure" caused by excessive deformation. As a result, the coordination law of internal force of pile anchor is revealed, and the anti sliding sharing mechanism is clarified. A design idea of the adjacent pile-anchor composite structure is proposed, which takes 0.2-0.3 times the remaining sliding force as the design value of prestressed anchor cable. The idea fully considers the anti sliding effect of prestressed anchor cables and reduces the design size of anti slide pile section, providing a theoretical support for optimization design of combined anti slide structure and saving project investment.

1. Introduction

A high slope may adopt adjacent pile anchor composite structure (Figure 1) to strengthen measures, which can not only rely on the passive reinforcement of anti slide piles to reduce the amount of slope excavation volume but also use the active reinforcement of prestressed anchor cables to limit slope deformation, reducing the design load of anti slide piles, making it widely cited in engineering practice [1, 2]. In addition, the rapid development of engineering technology has transformed most research results based on statics into dynamics [3, 4]. In recent years, the dynamic response characteristics of adjacent pile-anchor structures have become a research hotspot in slope engineering [5].

Le et al. [6] used Abaqus software to calculate and analyze the dynamic response of structure system of the supporting foundation pit under traffic loads and systematically studied the variation law of horizontal displacement of anti slide pile and axial force of anchor rod. Rainieri et al. [3] studied the response characteristics of embedded retaining wall under dynamic load and obtained a sensitivity coefficient of relevant model parameters to wall stability, which improved the existing design index of embedded retaining wall. Koca et al. and Nakajima et al. [7, 8] used the

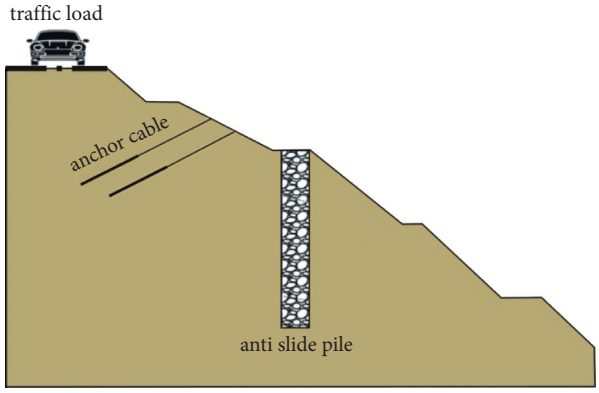

Figure 1: Schematic diagram of slope reinforcement with adjacent pile anchor composite structure.

principle of three-dimensional polar stereographic projection to analyze the dynamics of the bolt, thus obtaining the optimal anchoring angle of the bolt. Compared with the traditional method, the reliability of the conclusion is verified. Qu et al.[9, 10] studied the seismic response of prestressed anchor cable pile sheet wall through the shaking table model test, revealing the distribution law of soil pressure for prestressed pile sheet wall under earthquake action and providing a reliable basis for further understanding of the seismic performance and of the anti seismic mechanism of prestressed sheet-pile wall. Zhang et al. [11, 12] used the shaking table model test to study the seismic response characteristics of small angle layered inclined site in dip, strike, slope direction, and vertical direction of slope. The results have certain reference significance for seismic design of buildings on small angle layered inclined site.

This paper initially summarizes the research results in recent years. In the theoretical research of pile anchor structure, researchers systematically discuss the mechanical mechanism of reinforced structure from the aspects of elastic parameters, strength parameters, fracture damage parameters, and constitutive relations. However, the description of the anti sliding mechanism of pile-anchor structure is not yet completed, and the coordination characteristic of its internal force still lack of systematic research. As a result, the engineering design often ignores the effect of prestressed anchor cable on slope reinforcement [13], and the design size of anti slide pile becomes often too large to give full play to its advantages of slope reinforcement, resulting in a large number of engineering resources waste. Given the above shortcomings, this paper studies the anti sliding mechanism of adjacent anchor pile structure under traffic load. In the numerical simulation method, the time-domain analysis boundary condition of slope is improved, and the method of combining Lysmer's surface viscous boundary with traditional ground support boundary is adopted to reduce the large error caused by wave reflection in elastic boundary condition, so as to accurately describe the dynamic response mechanism of pile anchor structure. In this paper, a design idea of pile anchor adjacent composite structure is proposed, which fully considers the slope reinforcement effect of the prestressed anchor cable, to reduce the design size of anti slide pile section and to provide theoretical support for the optimal design of pile anchor composite structure.

2. Safety Analysis of Pile Anchor Composite Structure

2.1. Slope Engineering Features. The paper considers as a case study of the Chongqing Fuling Shizhu expressway construction project. Relying on K18 + 480~690 road section the right side slope engineering, the slope height is 32 m, the length is 168 m, and the area of sliding mass is about 10800 m^2. Stratum occurrence 323°∠32° intersects with slope occurrence 328°∠58° at a small angle, and the potential sliding surface is weak interlayer with poor stability, which belongs to plane sliding layered rock slope. The slope is excavated according to a four-level platform, and the height of each platform is 8 m. There is a reconstructed secondary road on the slope top. The plane and main sliding section of the slope are shown in Figure 2.

Due to the excavation of proposed expressway subgrade, the right side of the slope is free, and the stability of the slope is controlled by the dip angle of the rock stratum and the comprehensive shear strength between the layers. There are argillaceous intercalations in the slope. Under the induction of several factors such as atmospheric rainfall, outside loads, or hand-dug, the sliding surface further penetrates, thus making the strength of the layer decrease sharply. This aspect increases the risk of sliding for the slope along the weak interlayer, thus strongly decreasing its stability. In addition, the surface of the slope is affected by weathering and the layer is easy to be crushed, so the adjacent pile-anchor structure is used to reinforce the slope. Considering the traffic load on the slope top, it can be assumed that the load position is consistent with the free surface; in this condition, the safety of the pile-anchor composite structure should be analyzed.

2.2. Finite Element Model Size and Mechanical Parameters. The slope reinforcement scheme is as follows: the square anti slide pile is arranged on the second platform, with a length of 20 m, and the third slope surface is reinforced by double row prestressed anchor cables, with a length of 20 m and an anchorage section length of 10 m. The lithology of the slope is composed of sandstone, silty mudstone, and silty soil. The influence of weak interlayer on slope stability is simulated by establishing rock contact surface. Based on considering the slope size effect, the finite element numerical model of the slope is established, as shown in Figure 3. Through laboratory tests and relevant specifications, the mechanical parameters of rock mass and pile-anchor structure are shown in Table 1.

2.3. 3D Numerical Model. The scale of 3D finite element model is 1 : 1, and the rock stratum is modeled by solid element and obeys Coulomb–Mohr criterion. The model extends 24 m along the Z-axis, and the pile spacing is 6 m.

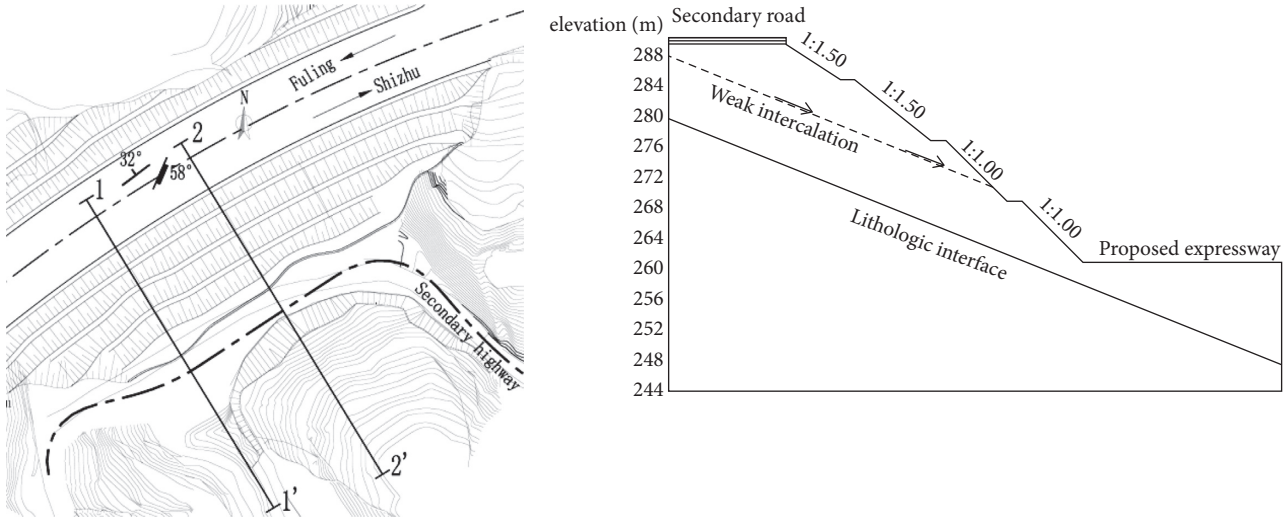

(a) (b)

Figure 2: Plane and section of K18 slope.

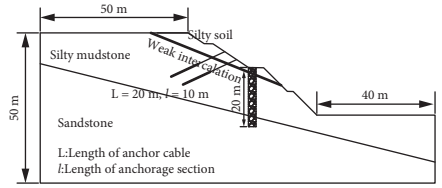

Figure 3: Section size of finite element model.

Table 1: Lithology and supporting structure calculation parameters.

Lithology and structure	Elastic modulus (MPa)	Poisson's ratio	Volume weight (kN/m^3)	Cohesion (kN/m^2)	Internal friction angle (°)	Prestress (kN)	Normal stiffness (kN·m)	Tangential stiffness (kN·m)
Sandstone	4609	0.17	25.18	1793	35.4	—	—	—
Silty mudstone	2306	0.29	25.71	1056	34.3	—	—	—
Silty soil	25	0.25	20	12.5	12.05	—	—	—
Anti slide pile	250000	0.2	24	—	—	—	—	—
Anchor cable	195000	0.3	78.5	—	—	500	—	—
Frame beam	10000	0.2	21	—	—	—	—	—
Weak intercalation	—	—	—	0	12	—	2.0×10^6	2.0×10^6

The anti slide pile and the frame beam of anchor cable are simulated by beam element, which is convenient to get the internal force value. The anchor cable is simulated by embedded truss [14–20], which is convenient to get the internal force variation characteristics, and the coupling with other element nodes cannot be considered. The finite element numerical software MIDAS GTS/NX is used for modeling. It is a professional geotechnical finite element analysis software application, especially good at slope stability analysis. The finite element numerical model is shown in Figure 4.

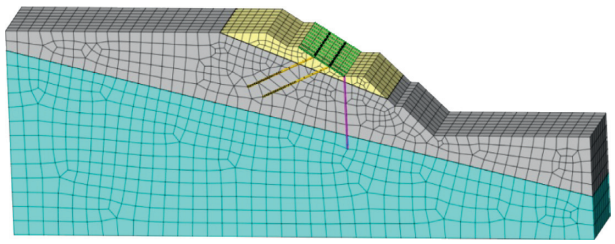

Figure 4: 3D finite element model.

2.4. Eigenvalue Analysis of Slope Dynamic Model. Free vibration analysis is called eigenvalue analysis. Through this analysis, the dynamic eigenvalues of the model, namely, natural frequency and mode shape, are obtained. In the slope dynamic finite element calculation, it is necessary to cut the

finite calculation domain from the natural geological body. The boundary conditions are imposed on the cut boundary, and then the dynamic analysis equation is established. Solving dynamic problems by using the principles and methods of structural dynamics [21–23]. Boundary conditions of the model are as follows: the bottom is a fixed boundary, x-direction displacement is constrained on both sides, and z-direction displacement is constrained longitudinally. In this paper, the elastic boundary is used to calculate the eigenvalue of the dynamic model, that is, the reaction coefficient of the elastic boundary is defined by the surface spring.

The calculation formula is as follows.

Horizontal reaction coefficient:

$$k_s = k_{s0} \cdot \left(\frac{P_s}{30}\right)^{-0.75}. \tag{1}$$

Vertical reaction coefficient:

$$k_h = k_{h0} \cdot \left(\frac{P_h}{30}\right)^{-0.75}, \tag{2}$$

where $k_{s0} = k_{h0} = \alpha E/30$, $P_s = \sqrt{A_s}$, $P_s = \sqrt{A_s}$, A_s and A_h correspond to the cross-sectional areas of each rock layer in the horizontal and vertical directions, respectively, E is the elastic coefficient, and α is taken as 1.0. The reaction coefficient of each rock stratum is calculated as shown in Table 2.

The natural frequency and mode shape are the natural characteristics of vibration system, and its generalized eigenvalue equation is

$$\left([K] - \omega^2 [M]\right)\{u\} = \{0\}, \tag{3}$$

where $[K]$ and $[M]$ are the stiffness matrix and mass matrix of the vibration system, respectively, and ω and $\{u\}$ are the natural frequencies and vibration modes.

The characteristic equation for determining the natural frequency is

$$\left|[K] - \omega^2 [M]\right| = 0. \tag{4}$$

After each natural frequency is obtained from equation (4), the corresponding natural mode can be obtained by substituting equation (3). Therefore, all eigenvalues ω_i and $\{u^{(i)}\}$ ($i = 1, 2, \ldots, n$, n is the degree of freedom) can be determined by using equations (1) and (2). The natural frequency shall meet $\omega_i \geq 0$ and $\omega_1 \leq \omega_2 \leq \cdots \leq \omega_n$.

According to the calculated reaction coefficient of each rock stratum foundation, the eigenvalue analysis results of slope dynamic model are shown in Table 3.

3. Dynamic Response Mechanism of Pile Anchor Composite Structure

Based on characteristic value of the slope dynamic model, the slope displacement and the pile anchor composite structure internal force at any time under traffic load can be calculated by analyzing the model in time domain. The dynamic equilibrium equation is as follows:

$$[M] \cdot u''(t) + [F] \cdot u'(t) + [K] \cdot u(t) = T(t), \tag{5}$$

Table 2: Reaction coefficient of every strata.

Lithology	Sandstone (kN/m^3)	Silty mudstone (kN/m^3)	Silty soil (kN/m^3)
Horizontal	90106	—	—
Vertical	136595/237440	158568/104815	—
Normal	81702	56612	1722

Table 3: Natural frequency and mode shape of slope dynamic model.

Vibration model	Frequency		Cycle
	rad/s	r/s	s
1	25.966776	4.132740	0.241970
2	27.351845	4.353181	0.229717
3	27.931513	4.445438	0.224950
4	28.654413	4.560492	0.219275
5	29.998140	4.774353	0.209452
6	33.324997	5.303838	0.188543
7	34.089333	5.425486	0.184315
8	35.464867	5.644409	0.177166
9	37.873245	6.027714	0.165900
10	38.598545	6.143149	0.162783

where $[M]$ is the mass matrix; $[F]$ is the damping matrix; $[K]$ is the stiffness matrix; $T(t)$ is the dynamic load; $u''(t)$ is the acceleration; $u'(t)$ is the velocity; and $u(t)$ is the relative displacement.

Because the elastic boundary conditions will produce large errors due to the reflection of waves, the time-domain analysis of slope dynamic model is solved by combining the curved viscous boundary proposed by Lysmer et al. [24–27] and the traditional ground support boundary, which can accurately describe the dynamic response characteristics of pile anchor composite structure.

3.1. Calculation of Viscous Boundary Damping Constant. In order to define viscous boundary conditions, it is necessary to calculate the slope model damping ratio in three dimensions. According to P wave (compression wave) and S wave (shear wave), the calculation formula of damping ratio is as follows:

$$P: \quad C_p = \rho \cdot A \cdot \sqrt{\frac{\lambda + 2G}{\rho}} = \gamma \cdot A \cdot \sqrt{\frac{\lambda + 2G}{\gamma \cdot 9.81}} = c_p \cdot A, \tag{6}$$

$$S: \quad C_s = \rho \cdot A \cdot \sqrt{\frac{G}{\rho}} = \gamma \cdot A \cdot \sqrt{\frac{G}{\gamma \cdot 9.81}} = c_s \cdot A, \tag{7}$$

where λ is the volume elastic coefficient (kN/m^2); G is the shear elastic coefficient (kN/m^2); c_p is the compression wave damping constant; and c_s is the shear wave damping constant.

$$\lambda = \frac{\mu E}{(1+\mu)(1-2\mu)};$$
$$G = \frac{E}{2(1+\mu)}, \tag{8}$$

Table 4: Damping constant of every strata.

Damping constant (kN·s/m)	Sandstone	Silty mudstone	Silty soil
P	3565.91	2815.85	247.31
S	2248.48	1531.40	142.78

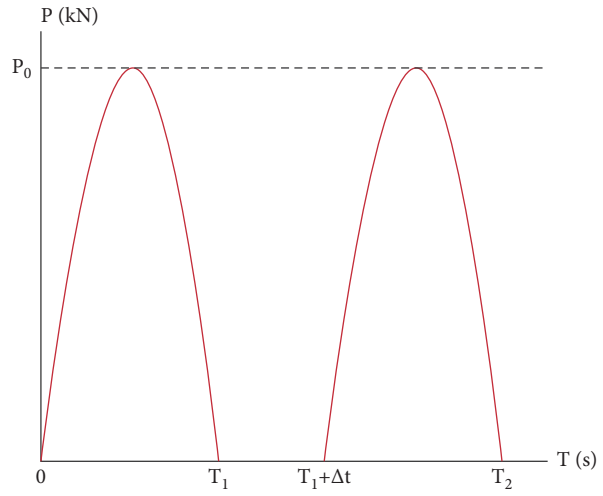

$$F(x,y,t) = \begin{cases} p_0 \sin\left(\frac{\pi}{T}t\right) & (0 \le t \le T) \\ 0 & (\text{else}) \end{cases}$$

Figure 5: Sine traffic load curve.

where μ is Poisson's ratio and E is the elastic coefficient (kN/m^2). The damping constants of each rock stratum obtained are shown in Table 4.

3.2. Time-Domain Analysis of Traffic Load Slope. In this paper, the direct integration method of linear time history analysis is used, and the natural frequency calculated by the aforementioned eigenvalues is substituted into equations (6) and (7) to calculate the corresponding mass and stiffness factors. For the traffic load on the slope top, when the car wheel passes through a certain point on the road surface at a certain speed, the change of the wheel load at that point is a process of first increasing and then decreasing, and its stress curve is a half-wave sine curve. The pressure effect of vehicle driving on the rock and soil mass under the road can be approximately simulated by repeated discontinuous half sine curve [28–31]. The sine load oscillogram is shown in Figure 5.

According to the requirements of "Specifications for Design of Highway Subgrades" JTG D30-2015, combined with the actual driving conditions of the reconstructed road, the driving load is taken as 50 kN/m. The traffic load is simulated by sine wave, and the maximum concentrated force of 500 kN is applied on the secondary road. In the figure, t is the action time of vehicle wheels, $\triangle t$ is the driving interval time of motor vehicles, and P_0 is the traffic load amplitude. The dynamic numerical model of time-domain analysis of slope under traffic load at the top of slope is shown in Figure 6.

3.3. Dynamic Response Mechanism of Slope Top Displacement. According to the calculation, the horizontal displacement and settlement response of the slope under the traffic load at the top of the slope are shown in Figure 7.

It can be seen from Figure 7 that the slope top secondary road produced displacement response in both the horizontal and vertical directions. Due to the support and anchoring effect of the anchor pile composite structure, the displacement does not penetrate down the weak interlayer to form a continuous sliding surface, and the slope is still stable. The maximum horizontal displacement and settlement are 7.48 mm and 15.16 mm, respectively.

Seven characteristic points (Figure 8) are selected at the central axis of the secondary road at the slope top. The horizontal displacement and settlement response curves of each point under traffic load are shown in Figure 9.

It can be seen from Figure 9 that the horizontal displacement and settlement response laws of each characteristic point are consistent under the traffic load at the slope top. The horizontal displacement response at point P_7 is the largest with a maximum amplitude of 7.45 mm, and the settlement at point P_6 is the largest with a maximum amplitude of 15.08 mm. As the slope is still stable, there is no irrecoverable horizontal displacement and settlement in the secondary road. After the end of the traffic load time history, the horizontal displacement and settlement of each characteristic point return to the initial state. There is no irrecoverable deformation of the slope.

3.4. Internal Force Response Mechanism of Pile Anchor Composite Structure. The internal force on the axis of the anti slide pile can be directly obtained by using the beam element simulation, that is, the difference between the pile back thrust and the resistance in front of the pile. The section of the maximum stressed pile is taken, and the internal force of the anchor pile composite structure under static load is combined. The internal force response curve of the pile-

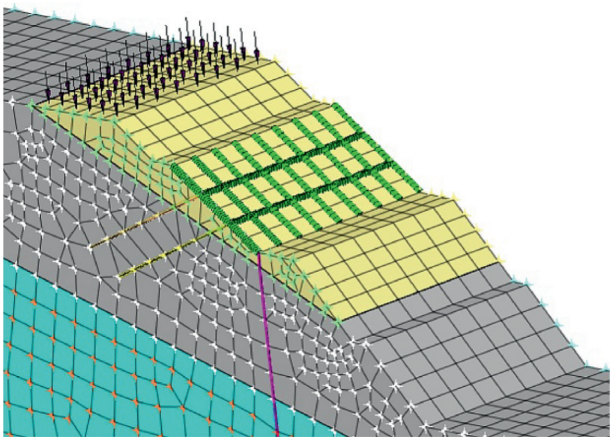

Figure 6: The dynamic model of slope time-history analysis

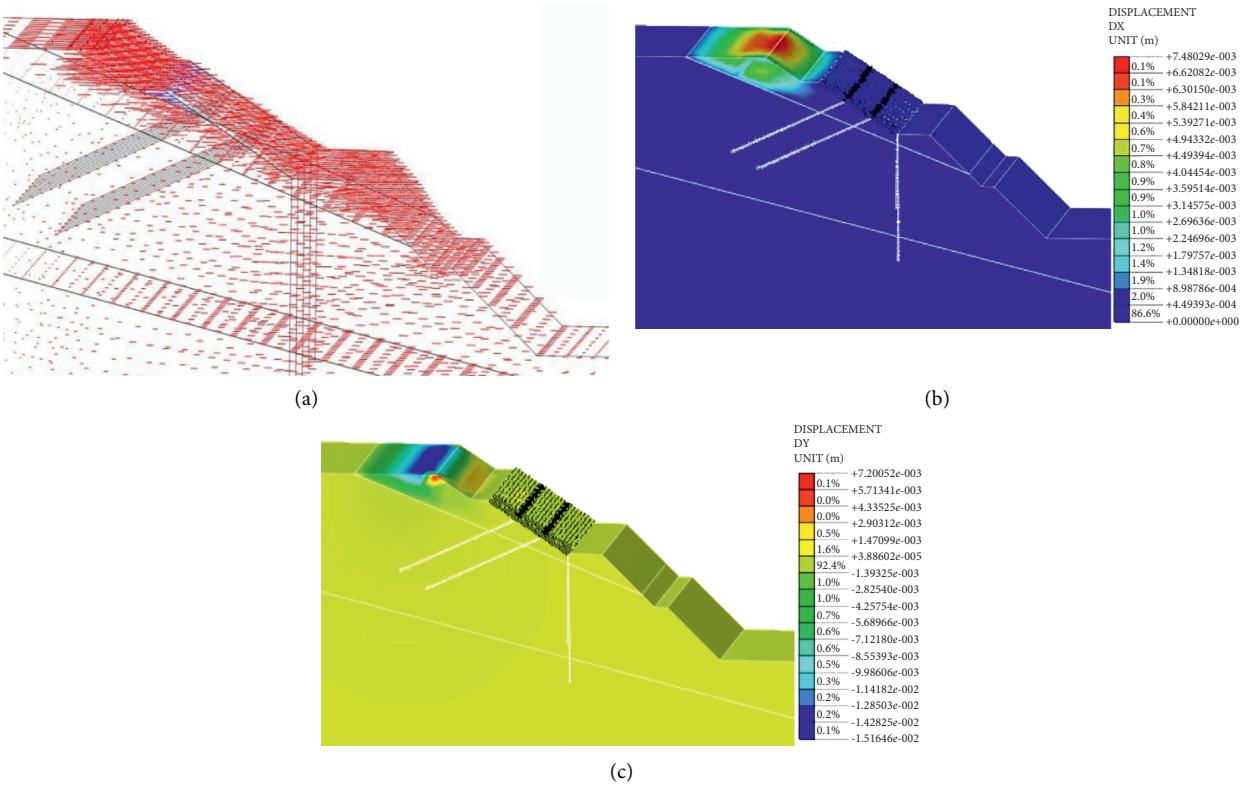

Figure 7: Characteristics of horizontal displacement and settlement of slope. (a) Displacement vector picture. (b) Horizontal displacement cloud picture. (c) Settlement cloud picture.

anchor composite structure under the traffic load on the slope top is shown in Figure 10.

According to Figure 10, the response law of the pile horizontal internal force and the slope horizontal displacement is consistent under the traffic load. During the initial stage of load, the pile internal force does not change too much, which is mainly related to the position of anti slide pile near the slope toe. With the change of traffic load time history, the anti slide pile can resist the slope slide by increasing the internal force. The anti slide pile's maximum internal force in the horizontal direction is 316.05 kN, the pile anchor composite structure's internal force reaches the maximum at t time, and the maximum anti slide pile internal force response increment caused by traffic load is 91.55 kN.

The results show that the position of the prestressed anchor cable is closer to the sliding surface, the internal force is more sensitive to the traffic load at the slope top, and the sliding of the slope is limited by increasing the internal force. Combined with Figure 7, the slope top is the concentration area of the maximum deformation. Therefore, in anti slide design of pile anchor composite structure, the prestress of

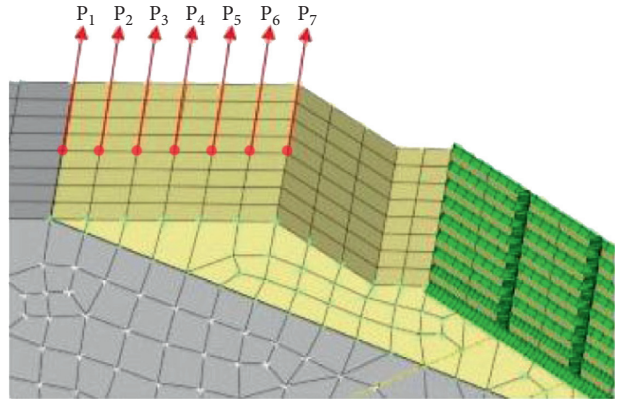

Figure 8: Characteristic point schematic diagram.

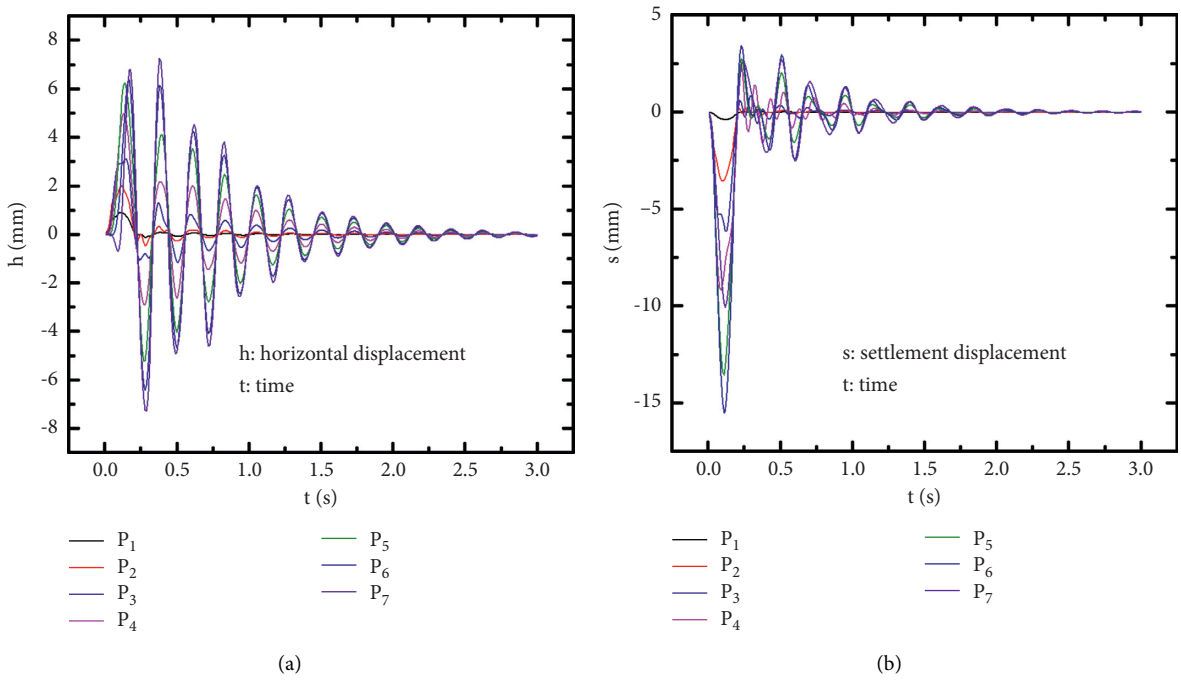

Figure 9: Horizontal displacement and settlement curve of slope time-history analysis.

the upper row anchor cable should be increased to avoid the "chain failure" of the anchor cable caused by excessive deformation. The maximum internal force of the lower row anchor cables is 143.69 kN, and that of the upper row is 119.30 kN. The internal force increment caused by traffic load is 33.19 kN and 8.29 kN, respectively. It can be seen that the anti sliding effect of the lower row cables is greater.

In engineering design, the reinforcement effect of prestressed anchor cable on slope in pile anchor composite structure is often ignored, which is only regarded as safety reserve [32]. According to the above analysis, the internal force increment of pile anchor composite structure under traffic load at the slope top is 124.74 kN, in which the internal force increment of anti slide pile accounts for 73.4%, and that of anchor cable accounts for 26.6%. In other words, the adjacent pile-anchor structure indirectly presents the coordinated sharing of the sliding force through the increase of their internal forces. Based on this, the adjacent pile-anchor structures indirectly show the coordinated sharing of the sliding force through the increase of their internal forces. In this way, a design idea of a pile-anchor combined structure is proposed, which is to use 0.2 to 0.3 times the remaining sliding force before the slope reinforcement as a preliminary. The design value of the prestressed anchor cable, by reducing the design size of the anti slide pile section, can provide a reference for the optimal design of the pile-anchor combined structure.

4. Joint Stabilization Slope Characteristics of Pile-Anchor Composite Structure

Based on the K18 + 480~690 section right side slope engineering of Fuling-Shizhu expressway construction project as an example, the earth pressure gauge and anchor cable stress meter (Figure 11) are used to monitor the internal force of

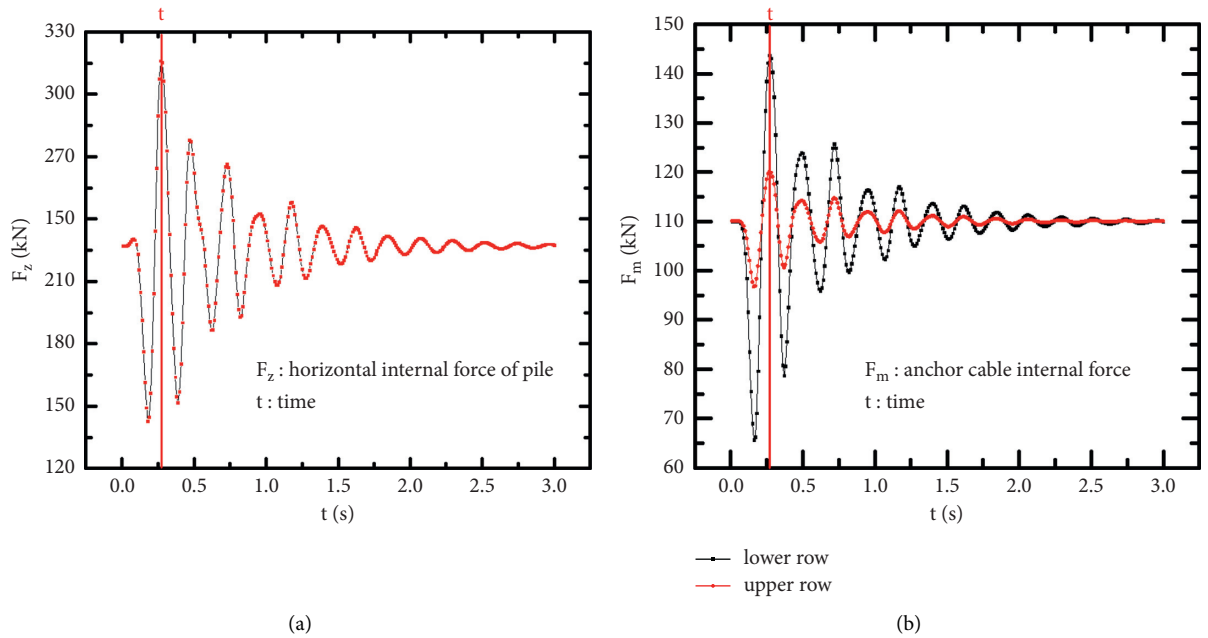

Figure 10: Internal force response curve of pile anchor composite structure.

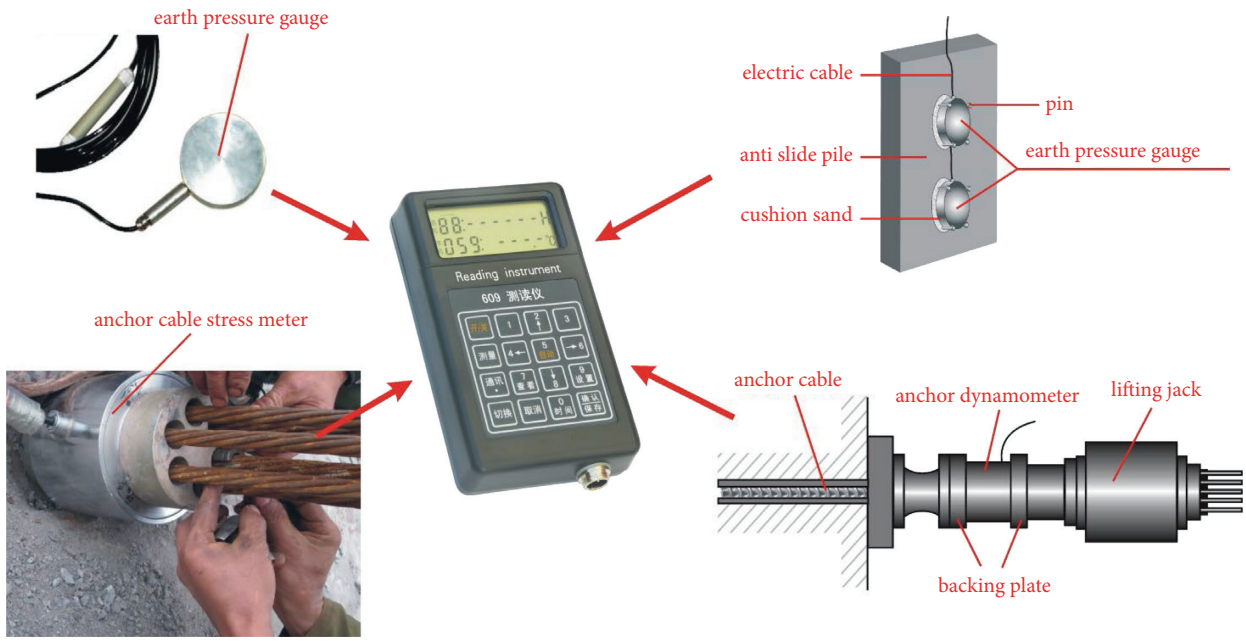

Figure 11: Anchor cable stress meter.

anchor pile composite structure for a long time. The rated tension of anchor cable sensor is 1~10000 kN, and the accuracy is ±0.02%; the accuracy of earth pressure gauge is ±0.1%.

According to the site construction conditions and the deformation characteristics of the slope, the section near the main sliding surface of the slope is selected. The internal force changes of the anchor pile combined structure are observed regularly. Figure 12 shows the section of instrument monitoring.

It can be seen from Figure 13 that the horizontal internal forces of the lower row anchor cables $M_{1\text{-}1}$, $M_{1\text{-}2}$ are 89 kN larger than those of the upper row $M_{2\text{-}1}$, $M_{2\text{-}2}$, and the internal force increment is 17 kN, which is four times the upper row anchor cable increment. Moreover, it shows that slope sliding extends downward from the top to the foot, and the anti sliding effect of the lower row anchor cables is significantly larger than that of the upper row. In addition, in the vertical direction, the internal forces of $M_{2\text{-}1}$ and $M_{1\text{-}1}$ near the main sliding surface are greater than those of $M_{2\text{-}2}$

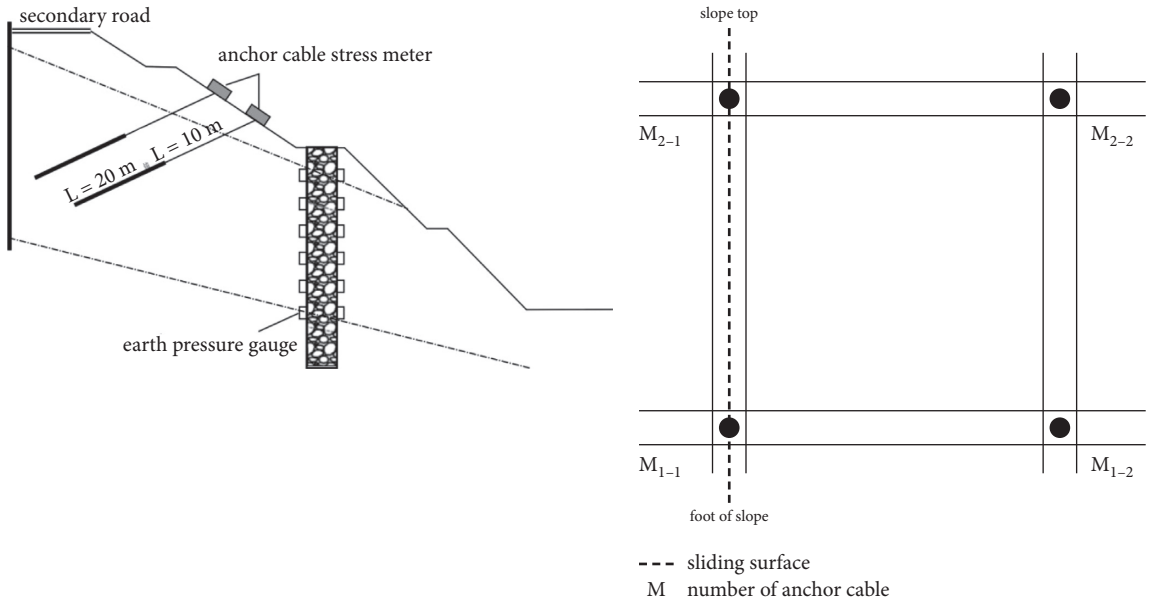

Figure 12: Monitoring point layout section of pile anchor composite structure. (a) Layout of earth pressure gauge. (b) Anchor cable number and layout plan.

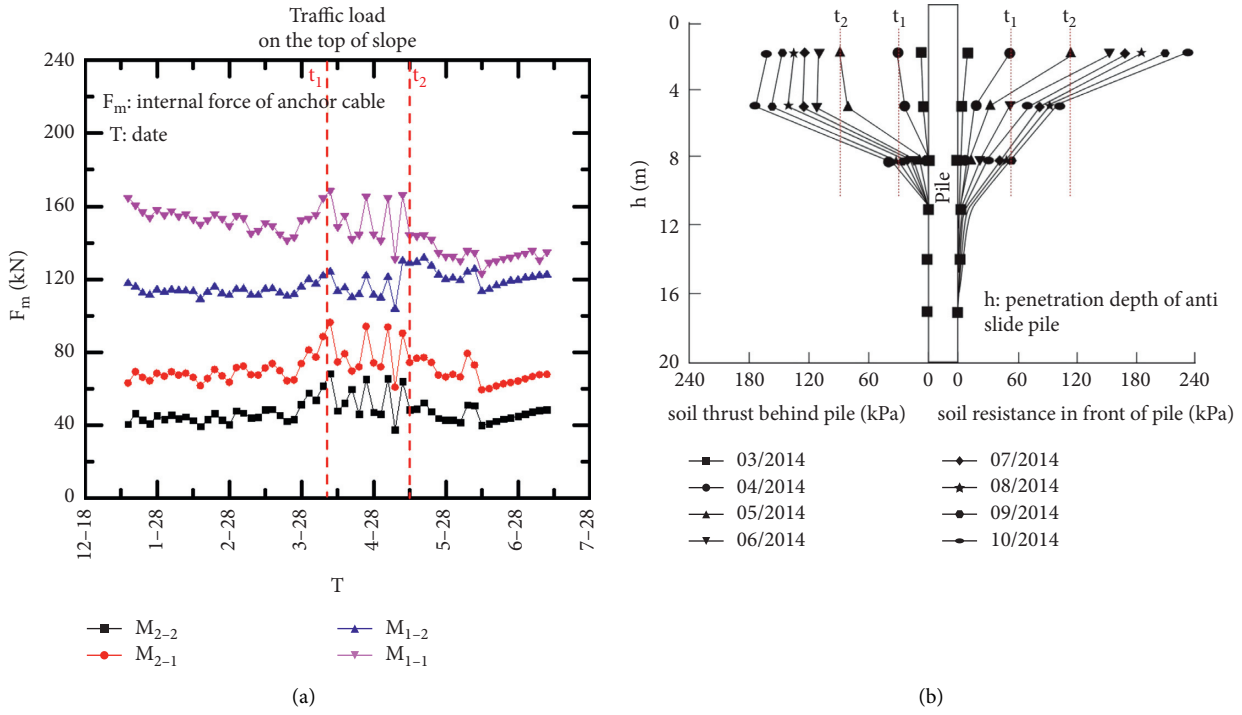

Figure 13: Internal force monitoring curve of anchor cable and anti slide pile. (a) Internal force monitoring curve of anchor cable. (b) Internal force monitoring curve of anti slide pile.

and $M_{1\text{-}2}$ on the other side away at the same level. During the time t_1~t_2 of traffic load on the slope top, the internal force of prestressed anchor cable has a sine wave which is consistent with the traffic load pattern. It shows that the internal force response of the anchor cable is produced, and the maximum internal force increment of the anchor cable is 24.58 kN during this period.

The thrust force behind the anti slide pile is less than the front resistance of the pile, and the internal force increment of the anti slide pile can be obtained by integrating the

difference between the two. According to the calculation, the maximum internal force increment of anti slide pile is 74.48 kN during t_1~t_2. The internal force increment of pile anchor composite structure caused by traffic load at the slope top is 99.06 kN. During the loading time, the internal force of pile and anchor is coordinated. Among them, 75.19% of the anti slide pile and 24.81% of the prestressed anchor cable bear the slope consolidation effect, which verifies the analysis results of finite element numerical simulation.

5. Conclusion

By establishing the dynamic model of adjacent pile-anchor structure combined under traffic load at the slope top, the collaborative mechanism of pile anchor adjacent composite structure was studied. In this paper, the time-domain equation error of traffic load dynamic model on the slope top is solved by combining Lysmer surface viscous boundary with traditional ground support boundary. The internal force response law of pile anchor composite structure is accurately described, and the internal force coordination mechanism is proposed. The main conclusions are as follows:

(1) The internal force increment of pile anchor composite structure under traffic load at the slope top is 124.74 kN, in which anti slide pile accounts for 73.4% and anchor cable accounts for 26.6%. The adjacent pile-anchor structures indirectly show the coordinated sharing of the sliding force through the increase of their internal forces. Through the coordination of internal forces, the combined structure exhibits the characteristics of efficiently resisting the sliding of the slope.

(2) The internal force increment of the lower row anchor cables is four times larger than that of the upper row, and the reinforcement effect of the lower row anchor cables is significantly larger than that of the upper row. Considering the displacement at the top of the slope is larger, it is suggested that in the anti slide design of pile anchor composite structure, the prestress of the upper row anchor cables should be increased to avoid excessive deformation of the lower row anchor cables, resulting in "chain failure."

(3) A design idea of pile anchor composite structure is proposed, which is 0.2~0.3 times the residual sliding force before slope reinforcement as the design value of prestressed anchor cable, which can reduce the design size of anti slide pile section and provide reference for the optimization design of pile anchor composite structure.

Data Availability

The data used to support the findings of this study are included within the article.

Conflicts of Interest

The authors declare that they have no conflicts of interest.

Acknowledgments

This research was supported by the National Natural Science Foundation of China (51908382), the National Natural Science Foundation of Hebei Province (D2020210004 and E2019210311), and the Independent Project of State Key Laboratory of Structural Mechanical Behavior and System Safety of Traffic Engineering, Shijiazhuang Railway University, China (ZZ2020-21).

References

[1] D. Li and L. Wang, "Synergism analysis of bedding slope with piles and anchor cable support under sine-wave vehicle load," *Advances in Materials Science and Engineering*, vol. 2016, pp. 1–8, 2016.

[2] X. Li, C. Li, and M. Bai, "Effect of pile spacing and pile arrangement on the stress of micropile supporting system," *Journal of Beijing Jiaotong University*, vol. 41, no. 4, pp. 47–54, 2017.

[3] C. Rainieri, A. Dey, G. Fabbrocino, and F. Santucci de Magistris, "Interpretation of the experimentally measured dynamic response of an embedded retaining wall by finite element models," *Measurement*, vol. 104, pp. 316–325, 2017.

[4] G. Fan and J. Zhang, "Determination of the seismic displacement relaxation zone in the reinforced slope by composite retaining structures," *Rock and Soil Mechanics*, vol. 38, no. 3, pp. 775–783, 2017.

[5] G. Fan, J. Zhang, and F. U. Xiao, "Large-scale shaking table test on dynamic response of bedding rock slopes with silt intercalation," *Chinese Journal of Rock Mechanics and Engineering*, vol. 34, no. 9, pp. 1750–1757, 2015.

[6] J. Le, Z. Qiu, and L. Zhang, "Analysis on dynamic response of the foundation pit supporting structure under traffic loads," *Chinese Journal of Underground Space and Engineering*, vol. 9, no. 6, pp. 1320–1325, 2013.

[7] M. Y. Koca, C. Kincal, A. T. Arslan, and H. R. Yilmaz, "Anchor application in Karatepe andesite rock slope, Izmir-Türkiye," *International Journal of Rock Mechanics and Mining Sciences*, vol. 48, no. 2, pp. 245–258, 2011.

[8] S. Nakajima, K. Abe, M. Shinoda, S. Nakamura, H. Nakamura, and K. Chigira, "Dynamic centrifuge model tests and material point method analysis of the impact force of a sliding soil mass caused by earthquake-induced slope failure," *Soils and Foundations*, vol. 59, no. 6, pp. 1813–1829, 2019.

[9] H. Qu, J. Zhang, and F. Wang, "Seismic response of prestressed anchor sheet pile wall from shaking table tests," *Chinese Journal of Geotechnical Engineering*, vol. 35, no. 2, pp. 313–320, 2013.

[10] H. Qu and J. Zhang, "Research on seismic response of anti sliding sheet pile wall by shaking table test," *Rock and Soil Mechanics*, vol. 34, no. 3, pp. 743–750, 2013.

[11] J. Zhang, G. Fan, and Z. Wang, "Large shaking table test on seismic response of inclined and layered site with small dip angle," *Rock and Soil Mechanics*, vol. 36, no. 3, pp. 617–624, 2015.

[12] J. Zhang, W. Liao, and Y. Ou, "Experimental research on mechanical behavior and bond performance of rock-anchor system subjected to repeated load," *Chinese Journal of Rock Mechanics and Engineering*, vol. 32, no. 4, pp. 829–834, 2013.

[13] X. Zhao, J. Huang, and Y. Zhou, "Joint reinforcement design method of tieback anchors on slope surface and anti slide piles at slope toe," *Journal of Southwest Jiaotong University*, vol. 52, no. 3, pp. 489–495, 2017.

[14] X. Zhao, C. Jiang, and Z. Xiong, "Study of transferring mode of prestressed force in singly anchored soil-like slopes," *Rock and Soil Mechanics*, vol. 31, no. 2, pp. 559–564, 2010.

[15] X. Zhao and Z. Xiong, "Study of transferring mode of prestressed force in frame-anchored soil-like slopes," *Rock and Soil Mechanics*, vol. 32, no. 7, pp. 2146–2152, 2011.

[16] H. Li, Y. Wang, and X. Sun, "Analysis and assessment of health status of unbonded prestressed anchors," *Chinese Journal of Rock Mechanics and Engineering*, vol. A01, pp. 2913–2924, 2019.

[17] Y. Chen, Y. Jin, and Y. Hu, "Research on prestress quantitative loss law of soft rock slope anchor cable," *Chinese Journal of Rock Mechanics and Engineering*, vol. 32, no. 8, pp. 1685–1691, 2013.

[18] L. Zhao, Q. Luo, and L. I. Liang, "Energy analysis method for slopes reinforcing with prestressed anchor cables based on minimum energy principle of instability state," *Rock and Soil Mechanics*, vol. 34, no. 2, pp. 426–432, 2013.

[19] Y. Wang, W. K. Feng, R. L. Hu, and C. H. Li, "Fracture evolution and energy characteristics during marble failure under triaxial fatigue cyclic and confining pressure unloading (FC-CPU) conditions," *Rock Mechanics and Rock Engineering*, vol. 54, no. 2, pp. 799–818, 2021.

[20] L. Bo, R. Bao, Y. Wang, R. Liu, and C. Zhao, "Permeability evolution of two-dimensional fracture networks during shear under constant normal stiffness boundary conditions," *Rock Mechanics and Rock Engineering*, vol. 54, no. 3, pp. 1–20, 2021.

[21] J. Lai, Y. Zheng, and Y. Liu, "Shaking table text study on anti slide piles and anchor bars of slope under earthquake," *China Civil Engineering Journal*, vol. 48, no. 9, pp. 96–103, 2015.

[22] Z. Tao, C. Zhu, M. He, and M. Karakus, "A physical modeling-based study on the control mechanisms of Negative Poisson's ratio anchor cable on the stratified toppling deformation of anti-inclined slopes," *International Journal of Rock Mechanics and Mining Sciences*, vol. 138, Article ID 104632, 2021.

[23] C. Zhu, M. He, M. Karakus, X. Zhang, and Z. Tao, "Numerical simulations of the failure process of anaclinal slope physical model and control mechanism of negative Poisson's ratio cable," *Bulletin of Engineering Geology and the Environment*, vol. 80, no. 4, pp. 3365–3380, 2021.

[24] G. Wang, C. Li, W. Chen, S. Xiong, M. Yu, and H. Zhang, "Mechanical characteristics of anchored slide-resistant piles under the condition of composite multilayer sliding bed," *Chinese Journal of Rock Mechanics and Engineering*, vol. 38, no. 11, pp. 2219–2230, 2019.

[25] Y. Yu, X. Liu, and Y. Liu, "Field experimental investigation on prestress loss law of anchor cable in foundation pits," *Rock and Soil Mechanics*, vol. 40, no. 5, pp. 1932–1939, 2019.

[26] R. Ganesh and J. P. Sahoo, "Uplift capacity of horizontal strip plate anchors adjacent to slopes considering seismic loadings," *Soils and Foundations*, vol. 56, no. 6, pp. 998–1007, 2016.

[27] E. Blanco-Fernandez, D. Castro-Fresno, J. J. Del Coz Díaz, and J. Díaz, "Field measurements of anchored flexible systems for slope stabilisation: evidence of passive behaviour," *Engineering Geology*, vol. 153, no. 8, pp. 95–104, 2013.

[28] D. Li, G. Yang, and W. Liu, "Dynamic index evaluation method of subgrade bearing capacity controlled by PFWD modulus," *China Civil Engineering Journal*, vol. 54, no. 6, pp. 117–128, 2021.

[29] Y. Xia and C. Chen, "Limit analysis of reinforced slopes with prestressed anchor cables considering energy dissipation due to deformation of inner friction," *Chinese Journal of Geotechnical Engineering*, vol. 39, no. 2, pp. 210–217, 2017.

[30] A. A. Jebur, W. Atherton, R. M. Alkhadar, and E. Loffill, "Nonlinear analysis of single model piles subjected to lateral load in sloping ground," *Procedia Engineering*, vol. 196, pp. 52–59, 2017.

[31] D. Li, L. Wang, B. Ge, and T. Shan, "Anti_slide analysis on the combination structure of anchor framework beam and pile in high slope sliding along lightly inclined strata," *Journal of Beijing Jiaotong University*, vol. 38, no. 4, pp. 137–142, 2014.

[32] X. Zhao, B. Wu, and D. Li, "Load calculation method for retaining wall between piles considering horizontal soil arching effects," *Chinese Journal of Geotechnical Engineering*, vol. 38, no. 5, pp. 811–817, 2016.